Impact-parameter structure of two-component absorptive models

Eliezer Rabinovici

Fermi National Accelerator Laboratory, Batavia, Illinois 60510 *
(Received 2 December 1974)

The impact-parameter structure of several two-component multihadronic production models is studied in the framework of elastic initial-state absorption. Models in which both the diffractive and the nondiffractive mechanisms lead to increasing cross sections are used to exemplify the nonlinear nature of absorption. It is found that absorptive effects may result in a large range of impact-parameter structures. On the one hand, diffractive components barely distinguishable from nondiffractive components are encountered and, on the other hand, absorption may lead to a "splitting" of the Pomeron into peripheral diffractive processes and central nondiffractive processes.

I. INTRODUCTION

Phenomenologically, it has been established that high-energy multihadronic production proceeds through two mechanisms.[1,2] The first is the dominant nondiffractive component which is of a multiperipheral nature and leads to decreasing n-particle production cross sections $\sigma_n(s)$. The second mechanism is of a diffractive nature and may involve Pomeron exchanges in a multiperipheral manner leading to asymptotic energy-independent $\sigma_n(s)$.

It has further been experimentally observed that the total cross section, σ_{tot},[3] increases with energy. This behavior is reproduced in various theoretical models.[4] A particular class of such models[5-8] invokes s-channel initial-state absorption to achieve an increasing σ_{tot} consistent with unitarity. However, these models usually involve only one production mechanism at a time.

In this work we attempt to investigate the features of various two-component models in the presence of absorption. Each component was constructed to lead to an increasing σ_{tot}. The nonlinear nature of absorption may induce additional structure when the two components are combined.

In Sec. II the initial-state elastic absorption procedure is reviewed, with emphasis on those of its properties which will be utilized latter. Two production models[6,7] that include absorption are reviewed in Sec. III, and they will serve as representatives of the diffractive and the nondiffractive components. In Sec. IV we analyze a simple two-component absorption model, and a classification of the possible solutions is performed by characterizing the different unabsorbed overlap functions with the help of two parameters: the coupling constant and the radius of the apparent unitarity violation. It is shown in Sec. V that this classification survives essentially unchanged

in a more complex two-component model based on the models presented in Sec. III. A case in which the nonlinear effects lead to an interesting structure in impact-parameter space is pointed out. They result in peripheral diffractive processes and central nondiffractive processes. In Sec. VI we conclude by surveying models in which diffraction is treated perturbatively.

II. THE ABSORPTIVE PROCEDURE

The application of multiperipheral dynamics to hadronic production processes has had considerable successes. Attempts have been made to describe both components of multihadronic production in terms of t-channel iterations. Multi-Regge exchanges (or elementary exchanges) have the short-range characteristic of the nondiffractive component and consequently predicted the scaling of the inclusive cross sections and the logarithmic increase of the average multiplicity of the produced particles. A multiperipheral scheme incorporating the exchange of an exclusive Pomeron is able to account for and predict many of the properties of high- and low-mass diffractive excitations.[9] However, it has been realized[10] that the multiperipheral scheme does not have built in s-channel unitarity constraints. In fact, elastic amplitudes constructed via unitarity by both Pomeron and non-Pomeron exchanges may violate the Froissart bound, and the approximate constancy (up to $\ln s$ factors) of the measured total cross sections must be traced to a special value of the coupling constant.

In order to overcome this difficulty, a way to tame any multiparticle output function was suggested[8,6] as follows: The unitarity equation in $\underline{b}$ (impact-parameter) space has the form

$$\text{Im} T_{el}(s, \underline{b}) = |T_{el}(s, \underline{b})|^2 + T_{inel}(s, \underline{b}), \tag{1}$$

where T_{inel} is the inelastic overlap function which

is the sum of all inelastic production at a fixed $\underline{b}$. Caneschi[8] has suggested that T'_{inel} as calculated from any model should be replaced in the unitarity equation [Eq. (1)] by T_{inel}. T_{inel} is related to T'_{inel} through

$$T_{\text{inel}}(s, \underline{b}) = f(S) T'_{\text{inel}}(s, \underline{b}) , \qquad (2)$$

where S is the S matrix. Assuming that the elastic amplitude is purely imaginary,

$$T_{\text{el}}(s, \underline{b}) = iA(s, \underline{b}) , \qquad (3)$$

the unitarity equation becomes

$$A = A^2 + f(S) T'_{\text{inel}} . \qquad (4)$$

Once T'_{inel} is given, this constitutes an equation for the elastic amplitude. A rather large class of functions $f(S)$ (Ref. 6) would ensure that for any T'_{inel}, $A(s, \underline{b})$ is always mapped in between the unitarity bounds:

$$0 \leqslant A \leqslant 1 . \qquad (5)$$

In a multiperipheral model one may try to associate the presence of $f(S)$ with absorptive corrections, in particular, with initial-state elastic rescattering. In this case $f(S)$ may have the form

$$f(S) = 1 - 2A . \qquad (6)$$

This suggestion neglects both inelastic diffractive absorption channels[11] and final-state rescattering corrections.[12] However, this over-simplified procedure not only restores unitarity but also allows for a self-consistent Pomeron.[6] We will thus pursue the results following from this type of implementation of absorption.

Denoting T'_{inel} by M and substituting Eq. (6) into Eq. (4), one obtains

$$A = A^2 + (1 - 2A)M . \qquad (7)$$

This equation can be explicitly solved for A:

$$A = \tfrac{1}{2}[2M + 1 - (4M^2 + 1)^{1/2}] . \qquad (8)$$

This solution has the following properties:

(a) It obeys the unitarity constraints [Eq. (5)] for every $\underline{b}$.

(b) If the inelastic overlap function increases indefinitely at a fixed $\underline{b}$ as a function of s, A reacts by approaching the value $\tfrac{1}{2}$:

$$A(s, \underline{b}) \xrightarrow[\substack{M \to \infty \\ (s \to \infty)}]{} \frac{1}{2}\left[1 - \frac{1}{4M(s, \underline{b})} + \frac{1}{64M^3(s, \underline{b})} + O\!\left(\frac{1}{M^5}\right)\right]. \qquad (9)$$

At each $\underline{b}$ where unitarity was threatened the scattering process is characterized by complete absorption. However, the absorption procedure does not insure that the Froissart bound will be respected. The short-range nature of strong in-

teractions must be manifest in the input overlap function M to insure that.

(c) In order to study the behavior of the inelastic processes after absorption one has to specify the manner in which the absorptive factor subdues an increasing M,

$$1 - 2A \xrightarrow[\substack{M \to \infty \\ (s \to \infty)}]{} \frac{1}{4M} - \frac{1}{64M^3} + O\!\left(\frac{1}{M^5}\right). \qquad (10)$$

Thus, the absorbed inelastic overlap function's contribution to the total cross section is given by

$$(1 - 2A)M \xrightarrow[\substack{M \to \infty \\ (s \to \infty)}]{} \frac{1}{4}\left[1 - \frac{1}{16M^2} + \frac{1}{64M^4} + O\!\left(\frac{1}{M^6}\right)\right]. \qquad (11)$$

We will make an extensive use of Eqs. (10) and (11).

(d) The elastic cross section is given by

$$A^2 \xrightarrow[\substack{M \to \infty \\ (s \to \infty)}]{} \frac{1}{4}\left(1 - \frac{1}{2M} + \frac{1}{16M^2}\right). \qquad (12)$$

In this scheme the elastic and inelastic cross sections approach a common limit as $M \to \infty$; however, the next-to-leading term in the total cross section will always originate from the elastic scattering.

(e) With the help of Eq. (8) one can study the behavior of the absorbed n-particle production cross section which is given by

$$\sigma_n(s, \underline{b}) = [(4M^2 + 1)^{1/2} - 2M]M_n(s, \underline{b}) , \qquad (13)$$

where $M_n(s, \underline{b})$ is the unabsorbed contribution of the n-particle production to the inelastic overlap function at a fixed $\underline{b}$. This result can be simplified by the approximation of Eq. (10). However, when M is of order unity, so is the absorptive factor.

Thus, given a certain model for the inelastic overlap function, one can find the detailed structure of the model after absorption has taken place. In order to clarify the effects that absorption has on the basic features of multiperipheral models two models[6,7] were already investigated. We next review these models which will later be utilized.

III. TWO ABSORBED MULTIPERIPHERAL MODELS

A. A self-consistent diffractive model[6]

The t-channel iteration of a fixed pole at $j = 1$ leads via unitarity to a pole above one in the elastic amplitude

$$A_{\text{el}}(j, t = 0) = \sum \frac{g^n}{(j-1)^n} = \frac{j-1}{j-1-g} , \qquad (14)$$

where g is a (positive) coupling constant. This

result neither respects unitarity bounds nor is self-consistent. Finkelstein and Zachariasen[6] have shown that in the framework of the absorptive procedure one can obtain a self-consistent Pomeron. One assumes that only the Pomeron is exchanged in the production process, and it is given by an expanding black disk of radius $R_0 Y$ (Y is the total rapidity),

$$T_{el} = \frac{i\,\theta(R_0^2\,Y^2 - b^2)}{2} \; ; \tag{15}$$

its j plane structure is

$$T(j, t) \propto \frac{1}{[(j-1)^2 - R_0^2 t]^{3/2}} \; . \tag{16}$$

Calculating the n-particle overlap function one obtains

$$m_n(Y, \underline{b}) = \left(\frac{g}{2}\right)^n \frac{[(R_0^2\,Y^2 - b^2)^{1/2}]^{3n-6}}{(3n-5)!} \, \theta(R_0^2\,Y^2 - b^2) \; . \tag{17}$$

The total overlap function is found to be[13]

$$M(Y, \underline{b}) = \frac{c_D \exp[(g/2)^{1/3}(R_0^2\,Y^2 - b^2)^{1/2}]\theta(R_0^2\,Y^2 - b^2)}{(R_0^2\,Y^2 - b^2)^{1/2}} \; , \tag{18}$$

where

$$c_D = \frac{g^{5/3}\,2^{-2/3}}{3} \; . \tag{19}$$

Once M is calculated, one can solve Eq. (7) for A_{el}. One finds that it is indeed given by Eq. (15) to first order, and that the Pomeron is self-consistent.

Using Eqs. (10), (13), and (18) one finds $\sigma_n(Y, \underline{b})$ to be

$$\sigma_n(Y, \underline{b}) = \frac{c'[(g/2)^{1/3}(R_0^2\,Y^2 - b^2)^{1/2}]^{3n-5}}{(3n-5)!}$$
$$\times \exp\left[-\left(\frac{g}{2}\right)^{1/3}(R_0^2\,Y^2 - b^2)^{1/2}\right]\theta(R_0^2\,Y^2 - b^2) \; . \tag{20}$$

Integrating over $\underline{b}$ one can show that $\sigma_n(Y)$ approaches a constant as the energy increases. This significant feature of diffractive processes comes about as follows:

$$\sigma_n(Y) \sim \int d^2b \, \frac{m_n(Y, \underline{b})}{M(Y, \underline{b})} \; . \tag{21}$$

Over most of the integration range $m_n(Y, b)$ has a power behavior in Y [Eq. (17)] while M is exponentially behaved [Eq. (18)]. The only way in which the cross section can survive at high energies is to be approximately energy independent at those $\underline{b}$ at which M ceases to be exponentially

behaved. M will always be of order unity at those b values where unitarity has not yet been violated (in this model, at b of the order $R_0 Y$). Thus the question of the survival of $\sigma_n(Y)$ reduces to the question of the behavior of $m_n(Y, b)$ at $\underline{b}$ of the order $R_0 Y$. In models (like this one) which exhibit a random walk in impact parameter the energy behavior of $\sigma_N(Y)$ can be traced to the energy behavior of the length of the random step (a).

In general the dispersion of the impact parameter after n steps is given by

$$\langle b^2 \rangle = na^2 \; . \tag{22}$$

In this model one has, due to the strong shrinkage,

$$\langle b^2 \rangle = n\left(\frac{Y}{n}\right)^2 \; . \tag{23}$$

For each fixed multiplicity n, $\langle b^2 \rangle$ increases like Y^2; $m_n(Y, \underline{b})$ can be approximated for this purpose by

$$m_n(Y, \underline{b}) \approx \exp\left(-\frac{b^2}{\langle b^2 \rangle}\right) \; . \tag{24}$$

At the critical $b \sim R_0 Y$, where M is always of the order one, $m_n(Y, \underline{b})$ is energy independent and allows for constant cross sections. The model also results with a rising plateau and long-range correlations; for a detailed study of this model, see Ref. 6.

B. A nondiffractive absorptive model[7]

Harari studied production models which may secure the intercept of the Pomeron at one and simultaneously relate the intercept of the nonleading trajectory α_R to the internal coupling constant g. The input was taken to be

$$m_n(Y, \underline{b}) = c_M \frac{(gY)^n}{n!} \frac{\exp(-b^2/4a^2 n)}{4a^2 n} \; , \tag{25}$$

where c_M reflects the external coupling constants and $4a^2$ is the slope of the form factor associated with each vertex. In terms of the j plane such an assumption represents the t-channel iteration of a fixed pole at $j = 1$:

$$m_n(j, t) = \left(\frac{g\,e^{4a^2 t}}{j-1}\right)^n \; . \tag{26}$$

The total inelastic overlap function is found to be

$$A_{inel}(j, t) = \sum_n m_n(j, t) = \frac{j-1}{j-1-g\,e^{a^2 t}} \; . \tag{27}$$

Approximating $e^{a^2 t}$ by its first two terms one obtains

$$M(Y, \underline{b}) \sim \frac{c \exp(gY - b^2/a^2 gY)}{a^2 gY} \; . \tag{28}$$

The $\underline{b}$ range over which unitarity would be violated without absorption expands like Y; so it is clear from Eq. (9) that the result is once again an expanding black disk. The total cross section increases like $\ln^2 s$. However, comparing the exchange of a cut [Eq. (16)] to an exchange of a pole also situated at one [Eq. (26)], we find that the asymptotic behavior of $\sigma_n(Y)$ is drastically changed:

$$\sigma_n(Y) \xrightarrow[s \to \infty]{} \frac{(gY)^n}{n!} \frac{(agY)^2}{(gY-n)} s^{-\mathscr{E}} . \tag{29}$$

In this case the length of the random step is constant (a^2), and the radius of the violation of unitarity has remained of order Y. Thus $m_n(Y, \underline{b})$ will be a decreasing function of energy at $b \sim Y$ and the cross section will be a decreasing function of the energy. (This result would also hold for a lower exchange with an intercept β as long as its coupling, g_β, is strong enough so that $g_\beta - 2\beta - 2 > 0$.) This type of energy behavior is one of the dominant features of nondiffractive hadronic production.

Experimentally, it has been established that there exist two components which are simultaneously responsible for the production of n particles. We have just presented two models which have the desired properties of each of the components. In the first model we have a $\sigma_n(Y)$ which tends to a constant while in the second model $\sigma_n(Y)$ decreases to zero as the energy increases. It may thus be interesting to study a model in which both mechanisms participate. Up to now each component was investigated independently of its companion. However, absorption is a nonlinear process and may lead to new features in a two-component model.

IV. TWO-COMPONENT ABSORPTION: A SIMPLE EXAMPLE

It is assumed that two mechanisms participate in the production process leading to "unabsorbed" inelastic overlap functions M_1 and M_2. One further assumes that each of the mechanisms separately would lead to an increasing total cross section.

The behavior of the two-component model in the presence of absorption is investigated by constructing the total driving term K, where K reflects the properties of M_1 and M_2:

$$K = M_1 + M_2 . \tag{30}$$

A is then obtained by solving Eq. (7) after replacing M by the total K. Since Eq. (7) is quadratic, one expects the model to have a different structure than each component separately. Several attempts to build the driving term K and investi-

gate the mutual interactions between its components will be discussed. In order to keep calculations as elementary as possible, we will deal first with a simple example which will nevertheless possess many features of more complicated models.

A large class of overlap functions is roughly characterized by two quantities:

(a) R—the radius over which the unabsorbed overlap function would violate unitarity (we will only deal with the case where the radius is logarithmically expanding with energy), which would also eventually reflect the magnitude of the total cross section should only one mechanism be operative.

(b) g—the internal coupling constant between the produced particles and the two adjacent t-channel exchanges in the process which builds up M.

The structure of a two-component absorptive model will thus be exemplified by using two overlap functions M_1 and M_2 which differ in their radii R_1, R_2 and their coupling constants g_1, g_2. Each would violate unitarity in the absence of absorption and lead to increasing cross sections

$$M_1 = \frac{g_1}{R_1^2 Y} \exp\left[\frac{g_1}{R_1^2 Y}(R_1^2 Y^2 - b^2)\right] , \tag{31}$$

$$M_2 = \frac{g_2}{R_2^2 Y} \exp\left[\frac{g_2}{R_2^2 Y}(R_2^2 Y^2 - b^2)\right] . \tag{32}$$

An exclusive model leading to such an overlap function was reviewed in Sec. III B.

Given this global information the problem addressed will be the following: What is the contribution of each mechanism to the total cross section at a fixed impact parameter $\underline{b}$?

Both mechanisms increase indefinitely, thus justifying the approximation stated in Eq. (10) for the absorptive factor. The two inelastic contributions I_1, I_2 resulting from absorption are given at fixed $\underline{b}$ by

$$I_1 \xrightarrow[Y \to \infty]{} \frac{M_1}{4K} , \tag{33}$$

$$I_2 \xrightarrow[Y \to \infty]{} \frac{M_2}{4K} . \tag{34}$$

The total inelastic contribution of the first inelastic mechanism to the total cross section is obtained by integrating Eq. (33) over the whole available $\underline{b}$ range,

$$I_1(Y) = \frac{Y^2}{4} \int_0^{R_1^2} d\eta^2 \frac{1}{1 + (g_2/g_1)(R_1^2/R_2^2)\exp[h(\eta)Y]} . \tag{35}$$

The upper limit of integration is the larger of R_1 and R_2; we have chosen it to be R_1. η is given by

$$\eta = \frac{|b|}{Y} ,\qquad (36)$$

and $h(\eta)$ is a function given by

$$h(\eta) = (g_2 - g_1) - \left(\frac{g_2}{R_2{}^2} - \frac{g_1}{R_1{}^2} \right) \eta^2 .\qquad (37)$$

A similar result is obtained for the second component. After absorption has been completed the elastic amplitude will, of course, turn out to be an expanding black disk, but one may still inquire how that black disk is built up from the production mechanisms at a fixed $\underline{b}$.

This structure will be governed by the behavior of the function $h(\eta)$. Whenever $h(\eta)$ has a positive definite sign over a certain range of η, that is, whenever M_2 is greater than M_1, only the mechanism which builds up M_2 will contribute, asymptotically, to the total cross section corresponding to that range of η. From the range where $h(\eta)$ is negative only contributions due to the first mechanisms will appear in the total cross section. The elastic cross section responds, for each $\underline{b}$, to the behavior of the inelastic cross section.

The analysis of the function $h(\eta)$ shows that one must distinguish between several cases:

(a) $R_1 > R_2$ and $g_1 \geq g_2$. In this case the first mechanism completely dominates the total cross sections for each $\underline{b}$.

(b) $R_1 = R_2$ and $g_1 > g_2$. In this case the consequences are the same as in (a).

(c) $R_1 = R_2$ and $g_1 = g_2$. In this case, both mechanisms have identical overlap functions and contribute equally for each $\underline{b}$.

(d) $R_1 > R_2$ and $g_2 > g_1$. In this circumstance, absorption results in a very interesting structure: The Pomeron in $\underline{b}$ space splits in two. For every value of $\underline{b}$ in the range $\eta_0 Y < b < R_1 Y$, it receives asymptotic contributions only from the first mechanism. For values of $\underline{b}$ in the range $0 < b < \eta_0 Y$ the absorbed overlap function is determined solely by the second mechanism. The transition point η_0 occurs at

$$\eta_0{}^2 = R_1{}^2 R_2{}^2 \frac{g_2 - g_1}{g_2 R_1{}^2 - g_1 R_2{}^2} .\qquad (38)$$

Thus η_0 is smaller than both R_1 and R_2.

The process with the larger radius and the smaller coupling constant is turned by absorption into a peripheral mechanism, while the process with the smaller radius and the larger coupling constant is confined to a circle of radius $\eta_0 Y$ around $b = 0$.[14] All other cases involve changing the roles of the two mechanisms. In Fig. 1 we show the detailed structure of the Pomeron in

case (d). The expanding black disk is composed of two parts, each of which consists of a "black" and a "gray"[14] region. One part is a peripheral expanding ring and the other is an expanding central disk.

Although all cases are logically possible, once the possibility of splitting the Pomeron has arisen one is tempted to inquire whether it is possible to construct a model which leads, under reasonable assumptions, to case (d). In the next section we will try to point out such a possibility.

V. TWO-COMPONENT ABSORPTION: DIFFRACTIVE AND NONDIFFRACTIVE MECHANISMS

In the former section a model consisting of two overlap functions having rather general features was investigated. In this section we try to study the fashion in which the results obtained are altered in a two-component model actually consisting of diffractive and nondiffractive components. Specifically, we will utilize the two models mentioned in Sec. III. The diffractive model leading to constant multiplicity cross sections is described by Eq. (18) and the nondiffractive model leading to decreasing cross sections is described by Eq. (28).

We proceed as in Sec. IV. Concentrating on the diffractive mechanism one obtains for the total inelastic diffractive contribution, σ_D,

$$\sigma_D = \frac{R_0{}^2 Y^2}{2} \int_0^1 \frac{dx}{1 + Kx \exp[f(x)(g_M/\gamma) Y]} ,\qquad (39)$$

where

$$K = \frac{c_M}{c_D}, \quad \gamma = \frac{a^2 g_M{}^2}{R_0{}^2}, \quad g_D = \left(\frac{\tilde{g}_D}{2} \right)^{1/3} ,$$

$$b = \eta R_0 Y, \quad x = (1 - \eta^2)^{1/2} ,\qquad (40)$$

and

$$f(x) = x^2 - \frac{\gamma}{z} x + \gamma - 1 .\qquad (41)$$

g_M is the coupling appearing in Eq. (28) and g_D is
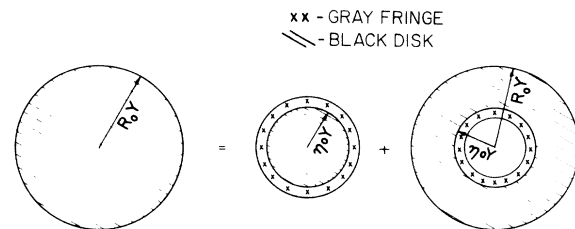

xx - GRAY FRINGE
\\\ - BLACK DISK

FIG. 1. The central and peripheral components of the Pomeron.

the coupling constant of Eq. (18).

The nondiffractive component violates unitarity in a radius $b < ag_M Y$, while the diffractive component violates unitarity in the range $b < R_0 Y$ (independent of g_D); thus a priori the largest absorbed $\underline{b}$ is given by

$$RY = \max(R_0 Y, ag_M Y) . \tag{42}$$

To obtain Eq. (39) we have assumed that $R = R_0$ but we will also discuss the other possibility.

The function $f(x)$ will determine [as the function $h(\eta)$ in Sec. IV] the dominant mechanism at each x. The function depends on two parameters:

(a) γ—which reflects the ratio of the radii of the two components;

(b) $1/z = g_D/g_M$ which is the ratio of the internal coupling constants of the two mechanisms.

The following cases occur (for more details, see Appendix A):

$I.\ \gamma \geqslant 1$.

(a) $z < 1$ $(g_M < g_D)$. In this case the black disk is fully diffractive.

(b) $z = 1$. Also in this case the disk is totally diffractive [unlike the simpler case (c) in Sec. IV].

(c) $z > 1$. In this case, when the nondiffractive coupling constant is greater than the diffractive coupling constant while the radius of the nondiffractive mechanism is smaller or equal to the diffractive radius, one finds that the Pomeron splits; it has a nondiffractive nucleus and diffractive periphery. [This occurs also for $\gamma = 1$, unlike case (d) in Sec. IV.]

II. For $\gamma > 1$ the results are similar; the main difference is in the region $1 < \gamma < \gamma_1$ (where $[\gamma_1, \gamma_2]$ is the interval of γ values over which the function $f(x)$ has no roots; see Appendix A). In that region the Pomeron consists of three parts: a nondiffractive nucleus, wrapped by a diffractive ring which is wrapped again by a nondiffractive ring.

Before presenting in detail all the possible configurations we will try to figure out what physical assumptions could help locate that section of the γ-z plane which is consistent with the knowledge we possess of production processes. In the absorption three radii are involved, two of which must be equal: ag_M is the radius of the nondiffractive processes, R_0 is the radius of the diffractive mechanism, and R is the radius of the resulting Pomeron.

If we now impose a self-consistency demand, that is, we will require that there exists only one Pomeron in the model, we obtain that R of the output Pomeron must be identical to R_0, the radius of of the input Pomeron. Thus self-consistency con-

strains us to the region of the γ-z plane where $ag \leqslant R = R_0$, that is, to the region $\gamma \leqslant 1$. If we further insist that the Pomeron built up by nondiffractive processes alone will also be identical to the Pomeron exchanged in diffractive processes we are led to the line $\gamma = 1$.

In order to complete our location in the plane one should try to estimate the expected value of z. If we accept the experimental indications that coupling constants characterizing nondiffractive processes are larger than those attached to diffractive processes, we are naturally led to the conclusion that physics could occur at the region $\gamma \leqslant 1$ and $z > 1$. However, this is just the region where the Pomeron splits. In that region the Pomeron is built up by a diffractive peripheral component and a nondiffractive component which is responsible for the more central collisions.

In Fig. 2 we demonstrate the various possible structures of the Pomeron in the γ-z plane.

For $z < 1$, motion along a line with a fixed z will describe a pure diffractive Pomeron as long as $\lambda \leqslant 1$. When γ exceeds 1, a nondiffractive ring is added to the Pomeron.

For $z > 1$ one finds that as γ increases, the nondiffractive nucleus also increases. In the interval $1 < \gamma < \gamma_1$ a nondiffractive ring appears and at γ greater than γ_1 the whole Pomeron turns nondiffractive. Motion along a line with a fixed γ shows the increase of the nondiffractive component as z increases. For $\gamma < 1$ the increase is felt only after z becomes larger than 1. When $1 < \gamma < 2$ the non-
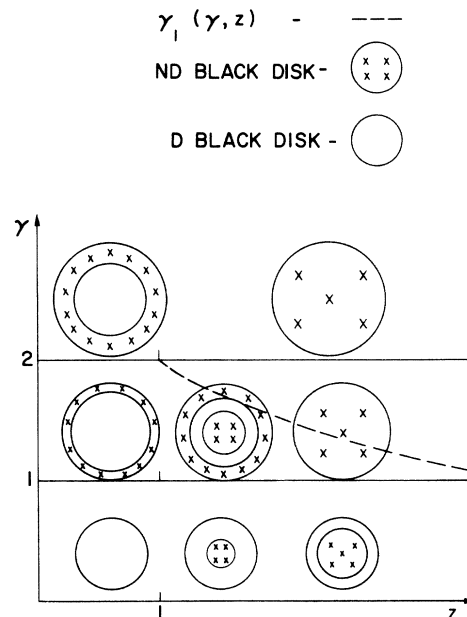

FIG. 2. The various possible structures of the Pomeron in the γ-z plane. $\gamma_1(\gamma, z)$ is defined in the Appendix.

diffractive component is a ring as long as $z < 1$.
When $z > 1$ it also appears as a nucleus forcing
the diffractive component into a ring. For $\gamma > 2$
and $z > 1$ the whole Pomeron turns nondiffractive.

For completeness we add some details on the
structure of the model in the case in which $\gamma = 1$
and the Pomeron splits. The total nondiffractive
inelastic cross section is given by

$$\sigma_M = R_0^2 \, Y^2 \left(1 - \frac{g_D^2}{g_M^2} \right), \tag{43}$$

and the diffractive contribution to the inelastic
cross section is

$$\sigma_D = R_0^2 \, Y^2 \frac{g_D^2}{g_M^2} . \tag{44}$$

One thus finds that the ratio of the cross sections
coming from the different components is

$$\frac{\sigma_M}{\sigma_D} = \frac{g_M^2}{g_D^2} - 1. \tag{45}$$

Experimentally, this quantity is much larger than
one. This may serve as another indication that
the assumption $g_M > g_D$ was reasonable.

Each multiplicity cross section $\sigma_n(Y)$ is com-
posed out of two components: one constant and
one decreasing with energy. Both components
sum, however, to increasing cross sections.

The special way in which absorption has taken
place affects the average multiplicity. The dif-
fractive processes were absorbed in the center
of the proton, thus losing the high-multiplicity
events. The nondiffractive processes were ab-
sorbed on the periphery; thus also they lost their
high-multiplicity events. The over-all average
multiplicity has decreased as a result of having
both components absorbing each other.

We have described in the last two sections the
results of absorbing a two-component model. Be-
tween the possible results we were led by self-con-
sistency arguments to the interesting "splitting"
of the Pomeron.

VI. TWO-COMPONENT MODELS: A PERTURBATIVE APPROACH

The main assumption involved in the model
presented in the former section was the ansatz
of the driving force K in terms of two overlap
functions, each representing a familiar model.
In this fashion no account was taken of production
processes initiated by exchanging simultaneously
both t-channel objects. In other words, we have
essentially neglected the coupling between a pole,
a black disk, and a produced particle. In this
section we will sketch the structure of a model
in which this coupling is treated perturbatively;

namely we will continue to assume the existence
of two production mechanisms. The nondiffractive
mechanism will again be represented by the mod-
el described in Sec. III B. The diffractive mech-
anism will include those processes in which only
one black disk is exchanged accompanied by a
chain of usual poles. Such a model may be of
interest if one infers from the ISR data[16] that
complete absorption is far from having been
developed. In such a case an exclusive exchange
of more than one or two black disks will be im-
possible for any energy available experimentally
for quite some time. The results will be pre-
sented in a qualitative manner and the approxima-
tions involved will be stated.

A. The overlap function

We begin by treating the diffractive component
independently and later add the effects of a two-
component model.

The general nature of a model is reflected in
the behavior of its overlap function. In this case
the overlap function is built out of two elements
(Fig. 3): a black disk (which for the time being
is confined to the end rungs), and from the pro-
cess in which a black disk collides with a proton;
one assumes that this collision is given essential-
ly by its nondiffractive component. (The black
disk behaves in a factorizable manner due to the
pion propagator which actually separates it from
the next exchange.[6]) Thus a black disk given by
$\theta(y_{12}^2 - b_{12}^2)$ and a pole given by Eq. (28') will com-
pete over the whole $(Y, \underline{b})$ space:

$$M(Y - y_{12}, \underline{b} - \underline{b}_{12})$$

$$= \frac{\exp[\, g(Y - y_{12}) - (\underline{b} - \underline{b}_{12})^2 / a^2 g(Y - y_{12})]}{a^2 g(Y - y_{12})} . \tag{28'}$$

y_{12} and b_{12}, are respectively, the difference in
rapidity and impact parameter between the first
and second produced particles. The black disk
is indifferent to the amount of the rapidity axis
it covers provided that it should always exceed
the amount of $\underline{b}$ that it has. Thus one finds that
the favorable configuration is one in which the
rest of the particles fill all the available rapidity
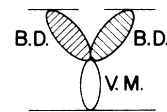and impact-parameter space and the black disk

FIG. 3. The unabsorbed diffractive overlap function.
B.D. is the exclusive black disk and V.M. is the total
nondiffractive component of the B.D.-proton scattering.

is left with $|\underline{b}_{12}| = y_{12} = 0$.

This indicates that the addition of a black disk to the production process will not radically alter the structure presented in Sec. III B. In particular, the cross sections σ_n that contributed the main bulk of the total cross section, at a fixed energy, before the addition of a black disk, will persist with their behavior. This does not mean that one cannot find quantities whose study will expose the existence of an exclusive black disk. For instance, following the behavior of the cross section for producing a fixed number of particles n as a function of energy, one discovers the influence of the exchanged black disk.

B. $\sigma_n(s)$ of the diffractive component

For simplicity we will follow the specific process in which one additional particle is produced by the two scattering particles. The production occurs by exchanging a black disk and a pole with intercept one (a different intercept will not change the result) (Fig. 4). The cross section is

$$\sigma_3(Y,\underline{B}) = c \int \theta(y^2 - b^2) e^{-(\underline{B}-\underline{b})^2} \, dy \, d^2 b. \tag{46}$$

As pointed out in Sec. III, the asymptotic fate of the cross section will be determined by its behavior at $|\underline{B}| \approx Y$. Both the pole and the black disk are indifferent to the fraction of the rapidity axis which they cover. Thus for $|\underline{B}| \sim Y$ the pole will stay at zero impact parameter and the black disk will be forced to extend all over the rapidity axis having $y = Y$. This configuration carries no energy penalty and actually resembles an exchange of a single black disk; the cross section is thus energy independent. This result clearly generalizes to any n.

The diffractive component thus leads, as desired, to constant cross sections. How can this be reconciled with the fact just stated that the total overlap function hardly changes by the addition of a black disk? What happens is that those σ_n that build up the $\ln^2 s$ of the total cross section at a fixed energy are practically unchanged by the exchange of the black disk. In other words, at each energy the sum of all cross sections which have already reached their asymptotic constant value is increasing slower than $\ln^2 s$. Such behavior is exemplified in Fig. 5, which
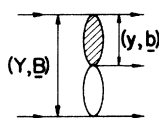
shows the behavior of $\sigma_n(s)$ as a function of n at a fixed energy. Most of the cross section comes from the region around the average multiplicity; cross sections in that region are far from their asymptotic value.

We have thus encountered a diffractive model whose gross features are very much like those of a nondiffractive model and whose distinct properties can be found only in rather fine details. This result should be contrasted with the behavior of other models for the diffractive components, such as models for single diffractive excitations.[9] In those cases the structure of the diffractive component is substantially different from that of the nondiffractive component. Absorption which allows a unitarity-violating unabsorbed overlap function is responsible for the difference.

C. Two- and more-component models

The diffractive component just described constitutes only part of the driving force, which will be completed only after adding the nondiffractive component. As a small difference exists between the two mechanisms, one expects both to contribute at every impact parameter. This can be verified in a more detailed model that involves some mathematical simplifications.[17] In this particular model both mechanisms contribute at each impact parameter; however, the ratio of their contributions is a function of $\underline{b}$. The larger the impact parameter, the larger the contribution of the diffractive mechanism to the total cross section. This is reminiscent of the peripheral structure of diffraction exhibited in the former sections.

The exclusive diffractive process was confined in the former analysis to the ends of the chain. The liberty to exchange the one black disk anywhere along the chain would result in a $\ln s$ enhancement of the diffractive processes relative to the nondiffractive processes. The output Pomeron would eventually reflect, at a very slow rate, only the diffractive processes. The addition of a finite number of exclusive black disks would bring about the same result.
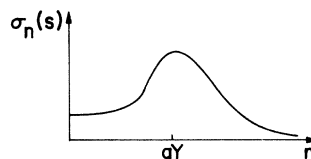
FIG. 4. The unabsorbed cross section for the diffractive production of three particles.

FIG. 5. The diffractive multiplicity cross sections $\sigma_n(s)$ as a function of n for a fixed s. The $\ln^2 s$ behavior of σ_{tot} comes from $n \sim gY$. The behavior at small n should be associated with already constant cross sections.

VII. SUMMARY

In this work we explored the effects of elastic initial-state absorption on several two-component models. The models describing both components were chosen to lead separately to increasing cross sections. We first utilized existing models for each of the components, and the mechanisms were characterized by the energy behavior of their multiplicity cross section, $\sigma_n(Y)$. It was found that these models offer a large range of solutions. Particular attention was paid to a case in which a "splitting" of the Pomeron had occurred. It was shown that by using self-consistency arguments and experimental evidence as to the dominance of nondiffractive processes one may be led to a solution in which absorption confines diffractive processes to be peripheral and nondiffractive processes to be central. The main interest in this case is that it illustrates some of the nonlinear effects of absorption. A "perturbative" two-component model was treated next, and the resulting diffractive process had many features in common with the nondiffractive mechanism. However, its special nature could be exposed by studying the asymptotically constant behavior of the cross section to produce n particles diffractively. The more components added the weaker becomes the signature of the nondiffractive mechanism on the output Pomeron. The models presented may eventually have phenomenological consequences; however, they are of an asymptotic nature. As long as a black disk behavior of the Pomeron is not observed experimentally,[16] there is no possibility of applying any of these models to the data. Finally one should add that the data do seem to support a split Pomeron[18]; however, whether this behavior persists up to the asymptotic region discussed in this paper is yet to be found.

APPENDIX

While investigating the properties of a two-component absorptive model including a diffractive and a nondiffractive mechanism, we found that the contribution of each mechanism at a fixed $\underline{b}$ [Eq. (39)] was governed by the behavior of the function $f(x)$ [Eq. (41)]

$$f(x) = x^2 - \frac{g_D}{g_M} \gamma x + \gamma - 1, \tag{A1}$$

where g_D and g_M were, respectively, the diffractive and nondiffractive coupling constants. γ was given by the ratio of the nondiffractive and diffractive radii [Eq. (40)]. One should remark that the x factor that appears in Eq. (39) is actually spurious at $x = 0$.[13]

The roots of the function $f(x)$ are

$$x_{1,2} = \frac{y\gamma \pm (y^2\gamma^2 + 4 - 4\gamma)^{1/2}}{2}, \tag{A2}$$

where $y = 1/z = g_D/g_M$. The equation has two roots for each z, except when γ is in the range

$$2z[z - (z^2 - 1)^{1/2}] < \gamma < 2z[z + (z^2 - 1)^{1/2}]. \tag{A3}$$

The edges of the interval were denoted γ_1, γ_2 and they are both functions of z.

We note the following cases:

(a) $z < 1$. In this case the large root x_2 is greater than 1 for every $\gamma > 0$. The small root x_1 is negative in the region $0 < \gamma < 1$, zero for $\gamma = 1$, and positive for $\gamma > 1$. Thus for each $\gamma \leqslant 1$, $f(x)$ is negative in the relevant interval $(0, 1)$. For $\gamma > 1$, $f(x)$ is positive in the interval $(0, x)$ and negative in the interval $(x_1, 1)$.

(b) $z = 1$. In this case x_1 increases from a negative value for $\gamma = 0$ to the value zero at $\gamma = 1$. For $\gamma > 1$, x_1 is positive and smaller than 1 until $\gamma = 2$. For $\gamma > 2$, $x_1 > 1$.

x_2 has a constant value 1 between $\gamma = 0$ and $\gamma = 2$; for $\gamma > 2$ one has $x_2 > 1$. Thus $f(x)$ is negative in the interval $(0, 1)$ for every $\gamma < 1$. For $2 > \gamma > 1$, $f(x)$ is positive in the range $(0, x_1)$ and negative in the range $(x_1, 1)$; for $\gamma > 2$ it is positive in the whole interval $(0, 1)$.

(c) $z > 1$. x_1 increases from a negative value at $\gamma = 0$ to zero at $\gamma = 1$. For $1 < \gamma < \gamma_1$, $0 < x_1 < 1$. For $\gamma_1 < \gamma < \gamma_2$, x_1 does not exist. For $\gamma > \gamma_2$, x_1 decreases but is always above 1. x_2 decreases from 1 at $\gamma = 0$ to $0 < x_2 < 1$ for $\gamma < 1$. For $\gamma > \gamma_2$, $x_2 > 1$. Thus $f(x)$ is negative in the interval $(0, x_1)$ and positive in $(x_1, 1)$ as long as $\gamma > \gamma_1 > 1$; for $\gamma > \gamma_2$, $f(x)$ is positive in the interval $(0, 1)$. The line appearing in Fig. 2 describes the relation between γ_1 and z.

We conclude by remarking that the situation in the case $z > 1$ is actually more involved. In principle g_M and g_D could be estimated by measuring the average multiplicities of diffractive and nondiffractive events. However, it seems that the Pomeron is still far from behaving like a black disk even at ISR energies.[16] This means that the displacement of the pole above one is small while multiplicities are not small. One may perhaps regard nondiffractive processes as originating from an exchange of a Reggeon of intercept α_M lower than one, but with a larger coupling constant g_M such that

$$\epsilon = 2\alpha_M - 2 + g_M > 0.$$

In this case absorption may still be small, while $\langle n \rangle$, whose behavior is governed by g_M, is large. In this Appendix we also analyze the case where a new parameter ϵ has been introduced.

In this case the function $f(x)$ is

$$f(x) = x^2 - \frac{g_D}{g_M} x + \frac{\epsilon \gamma}{g_M} - 1. \tag{A4}$$

We will deal with the case $\gamma = 1$. The roots x_1, x_2 are

$$x_{1,2} = \frac{y \pm (y^2 - 4k + 4)^{1/2}}{2}, \tag{A5}$$

where $y = g_D/g_M$ and $k = \epsilon/g_M$. If $0 < k < 1$, then for each $0 < y < k$, one has $0 < x_2 < 1$ and $x_1 < 0$. Thus in this range where $\epsilon > g_D$, $f(x)$ is negative in the interval $(0, x_2)$ and positive in $(x_2, 1)$. Thus once again the Pomeron splits.

*Operated by Universities Research Association Inc. under contract with the United States Atomic Energy Commission.

[1]For a review of two-component models see, e.g., H. Harari, in *Proceedings of the 14th Scottish Universities Summer School in Physics* (Academic, New York, 1974), and references therein.

[2]H. Harari and E. Rabinovici, Phys. Lett. <u>43B</u>, 49 (1973); C. Quigg and J. D. Jackson, NAL Report No. NAL-THY-93, 1972 (unpublished); W. Frazer, R. Peccei, S. Pinsky, and C.-I Tan, Phys. Rev. D <u>7</u>, 2647 (1973); K. Fiałkowski and H. Miettinen, Phys. Lett. <u>43B</u>, 61 (1973).

[3]U. Amaldi *et al.*, Phys. Lett. <u>30B</u>, 766 (1973); S. R. Amendolia *et al.*, *ibid.* <u>44B</u>, 119 (1973).

[4]For a review, see, e.g., F. Zachariasen, Caltech Report No. CALT-68-385 (unpublished).

[5]K. Gottfried and J. D. Jackson, Nuovo Cimento <u>34</u>, 735 (1964).

[6]J. Finkelstein and F. Zachariasen, Phys. Lett. <u>34B</u>, 631 (1971); L. Caneschi and A. Schwimmer, Nucl. Phys. <u>B44</u>, 631 (1972).

[7]H. Harari, Phys. Lett. <u>51B</u>, 479 (1974).

[8]L. Caneschi, Phys. Rev. Lett. <u>23</u>, 254 (1969).

[9]H. Harari and E. Rabinovici, Ann. Phys. (N.Y.) (to be published); D. Snider and W. Frazer, Phys. Lett. <u>45B</u>, 136 (1973); R. G. Roberts and D. P. Roy, *ibid.* <u>46B</u>, 201 (1973); D. Horn and M. Moshe, Nucl. Phys. <u>B65</u>, 112 (1973); D. Amati, L. Caneschi, and M. Ciafaloni, *ibid.* <u>B62</u>, 173 (1973).

[10]J. Finkelstein and K. Kajantie, Phys. Lett. <u>26B</u>, 305 (1968).

[11]R. Blankenbecler, Phys. Rev. Lett. <u>31</u>, 964 (1973); R. Blankenbecler, J. R. Fulco, and R. L. Sugar, Phys. Rev. D <u>9</u>, 736 (1974).

[12]M. Ciafaloni and G. Marchesini, Nucl. Phys. <u>B71</u>, 493 (1974); CERN Report No. CERN-1932, 1974 (unpublished); A. Schwimmer, Nucl. Phys. <u>B75</u>, 446 (1974).

[13]Equation (18) is actually an approximation for large $(Y^2 - B^2)^{1/2}$. In the exact result no singularity occurs at $B = Y$.

[14]In fact there is some additional structure to this split. The behavior of a mechanism for an impact parameter where it is nondominant is described by a decreasing power of energy; however, the total nondominant contribution is ln$s$. The origin of this contribution can be traced to a shrinking fringe, converging to the radius $\eta_0 Y$. A fringe with a similar contribution was observed in Ref. 15.

[15]H. Cheng and T. T. Wu, Phys. Rev. Lett. <u>24</u>, 1456 (1970).

[16]U. Amaldi, J. Phys. Suppl. <u>C1</u>, 241 (1973).

[17]The main approximation consists of dealing mainly with the behavior of $\sigma_n (Y, B)$ at $|B| \sim R_0 Y$. The physical motives for this were outlined in Sec. III.

[18]For a review of the experimental evidence of the two-component structure of the Pomeron, see G. L. Kane, Report No. UM HE 73-10 (unpublished) (invited talk at the ANL Symposium on the Pomeron).